Fundamental Knowledge of Fatigue Fracture

by
J. C. Grosskreutz
Metallurgy Division
National Bureau of Standards
Washington, D. C. 20234

Abstract

The frontiers in our knowledge of fatigue are reviewed here with the aim of describing the current status and the opportunities for fresh approaches to increase our understanding. The principal opportunity is to quantify that which we already know qualitatively. Throughout the paper an attempt is made to connect fundamental knowledge to the technical problems in fatigue which still remain vexing and unsolved.

1. Introduction

The subject of fatigue mechanisms has been reviewed rather thoroughly during the past several years (1,2). Rather than to repeat or update these reviews, this paper will attempt to define the frontiers of research in fundamental fatigue knowledge. First, this approach will be applied within the classical framework of the fatigue sequence: hardening/softening, crack initiation, and crack propagation. In subsequent sections, we will turn to the application of our fundamental knowledge to the more practical or technical problems in fatigue failure.

With a few exceptions, we have today a rather good qualitative knowledge of the fatigue process. We can describe it in words and define some of the important microstructural changes which occur during fatigue, but we are only beginning to arrive at a quantitative description. If the frontiers of fatigue research could be expressed in a single sentence, it would be: to quantify that which we already know qualitatively.

2. Frontiers in the search for fundamental knowledge of fatigue fracture.

In this section, the discussion will be arbitrarily confined to monolithic materials (as opposed to composites) and to constant amplitude loading conditions. The more advanced materials and the technically important problem of variable amplitude loading will be discussed in Section 3.

2.1 Fatigue hardening/softening

The cyclic stress-strain curve, which is a plot of the peak saturation flow stress vs. the applied strain amplitude, represents the best means for displaying the steady-state fatigue response of a material. It is important to realize that the cyclic stress-strain curve can be quite different from the tensile (or compressive) curve. Figue 1 illustrates this fact. This important curve can be represented empirically by the expression

$$\sigma_a = K' \, (\Delta\varepsilon_p/2)^{n'} \qquad [1]$$

where σ_a and $\Delta\varepsilon_p/2$ are the steady-state, or equilibrium (saturation) values of the applied stress and plastic strain amplitudes, respectively. K' is a material constant and n' is the cyclic strain hardening exponent. Compilations of K' and n' for various materials are beginning to appear (3). Recently, Lukas and Klesnil have reported cyclic stress-strain curves for Cu and brass at very low amplitudes (4).

Many studies reported in the literature have documented the microstructural changes and dislocation structures which result from fatigue hardening/softening (1). One of the great needs is to assimilate the existing data and to design careful experiments which will provide the missing information so that a quantitative theory of

hardening/softening can be constructed to replace the empirical relationship Eq.[1]. Two recent experimental observations have aided materially in constructing a model of the equilibrium hardening state in pure copper at high strain amplitudes. They merit brief comment.

The influence of point defects and their clusters on the equilibrium flow stress in fatigued materials has been a subject of much speculation (1). The experimental fact that the temperature dependence of the flow stress of fatigue hardened specimens lies between that of unidirectionally deformed and neutron irradiated specimens is the strongest evidence that the hardening is partially controlled by some thermally surmountable barrier for dislocations. In the case of copper, the ratio of the flow stresses at 300°K to that at 78°K for the three cases is:

	$\sigma(300°K)/\sigma(78°K)$	
tension(5)	fatigue(6)	neutron irradiated(5) (10^{17} nvt)
0.95	0.88	0.62

In (6), equilibrium flow stresses were determined for copper single crystals over the temperature range 78-300°K for a variety of cyclic strain amplitudes, and the size and space distribution of point defect clusters were determined by transmission electron microscopy. These two observations, together with an analysis based on the approach of Frank, et. al (7) for neutron-hardened copper, allowed the authors to select a consistent model for fatigue hardening. If the equilibrium flow (shear) stress is subdivided according to

$$\tau = \tau_\mu + \tau^* \qquad [2]$$

into an athermal (τ_μ) and a thermal (τ^*) component, then τ^*/τ was determined to be 15-25% depending on the strain amplitude. Furthermore, τ is determined by the to-and-fro shuttling of dislocations within regions of low dislocation and defect cluster density (cells) where they must overcome long-range internal stress (athermal) and short range stresses (thermal) provided by interaction with point defect clusters.)

This model has been further confirmed by the transmission electron micrographs obtained by Mughrabi from fatigued copper crystals for which the dislocation structure had been "frozen in" by neutron irradiation in the stress-applied state (8). Figure 2 illustrates the presence of screw dislocations in the cell interiors.

The whole subject of fatigue softening and the stability of various microstructures under cyclic loading has been almost totally unexplored. A brief review of what is known has been given in ref. (9).

An equally important frontier is the stability of the fatigue hardened state. Neumann (10) has shown that strain "bursts" occur when copper is fatigued under a slowly rising stress amplitude. These bursts last for about 50 cycles and the specimen is quiescent again until the stress becomes high enough to initiate another burst. Theoretical studies of the stability of dislocation dipoles (which are present in large numbers in fatigued copper) have shown that microstructures containing dipoles are likely to be unstable against the injection of a few free dislocations (11). In such a case, an avalanche of dislocations could be expected as the dipole clusters decompose. Relating this phenomenon to the processes of crack initiation and crack growth should provide some fascinating insights into fatigue.

Two final areas that require much new research effort a) the effect of strain rate, and b) the effect of temperature on cyclic stress strain response. Our present knowledge is scanty. Hancock

and Benson (12) have measured the dependence of n' on strain rate and find the relation shown in Figure 3 for 7075 aluminum alloy. This dependence predicts, according to the equations of Tomkins (13), that low cycle fatigue life and crack growth rates should increase and decrease, respectively, as $\dot{\varepsilon}$ is increased.

The effects of temperature on the cyclic stress-strain curve were reported recently by several authors at the 1972 Symposium on Fatigue at Elevated Temperatures held at Storrs, Connecticut (14). Tomkins found that for stainless steel, values of the equilibrium stress for a given strain amplitude were lowered as temperature was increased, the strain rate being held constant (Fig. 4).

2.2 Crack Initiation

A perplexing, and little understood problem is that of crack initiation in high strength materials under long life fatigue conditions. For example, microcracks ≥ 1 μm in length in notched 7075-T6 aluminum are not observed until after 95% of a nominal 10^6 cycle fatigued life has elapsed (16). Cracks then appear suddenly at inclusions without benefit of observable slip or plastic deformation of the surface. Moreover, so-called "slipless" fatigue crack initiation has been observed in long life fatigue of titanium alloys, again after a long period of unobservable deformation on the surface. Cracks ≥ 1 μm occurred in grains of Ti-6Al-4V after ~ 45% of a total life of 10^6 cycles and grew in the direction of maximum shear, (17). (At shorter lifetimes and higher stress amplitudes, classical slip-band initiation occurs.) In commercially pure titanium, MacDonald and Wood (18) observed that cracks appeared in grains otherwise devoid of slip when cycling was conducted in the elastic range, (Fig. 5). While in the cases of 7075-T6 Al and Ti-6Al-4V, the crack origins could be defined as inclusions and α/β interfaces, respectively, no such defects or interfaces were present in the case of pure Ti, and the cracks simply appeared transgranularly in the direction of maximum shear. The basic question is: "what is happening during the long quiescent period during which no observable plastic deformation is observed to preceed the appearance of a crack in these materials"?

The mechanisms and sites for crack initiation at elevated temperatures have not received much attention except for a few, specific materials. A rather general impression exists that crack initiation takes place predominately at grain boundaries for $T \geq 0.4\ T_m$, but it is not clear whether this impression would stand under critical inspection. The age-hardened, nickel base super alloys, because of their application to high temperature, turbine usage, have been explored in detail (19). For example, wrought Udimet 700 deforms in a planar slip mode below 1400°F, and crack initiation occurs in slip bands or at twin boundaries. The transition from transgranular to intergranular initiation usually occurs as temperature is increased, but the specific temperature is a function of test conditions, type of alloy, and its structure.

Perhaps the most important and most difficult frontier in crack initiation research is clarification of the effects of environment on mechanisms and rates of initiation. For our brief treatment here, we divide the discussion into two parts, the effects of environment *per se*, and the contributory problem of surface films.

Laird and Duquette, in their review of crack initiation, have concluded (15) that the effect of gaseous environments on crack initiation rates is small, especially compared to the effect on crack growth. Grosskreutz has presented data on the number of cycles, N_o, to initiate a crack 10 μm deep in commercially pure aluminum

fatigued either in 2×10^{-6} Torr vacuum or in 100% relative humidity air (20). The ration $(N_o)_{vac}/(N_o)_{air}$ was 1.7, which is rather small in terms of its effect of total life. On the other hand, the presence or absence of gaseous environments can drastically affect the mechanism of crack initiation (20).

Aqueous environments are known to play a significant role in fatigue crack initiation. Many mechanisms have been proposed such as pitting, preferential dissolution at plastically deformed sites, protective film destruction, and surface energy reduction. We will not discuss these various mechanisms here (the reader is referred to ref. (15)), but will state only that, whatever the mechanism, there is serious need for quantitative data concerning crack initiation rates (N_o/N_f) for specific material-environment couples. Concurrent with such experiments, the corrosion rates below which quantitative effects on crack initiation cease to exist should be recorded, so that predictions can be made about corrosion fatigue susceptibility.

A more subtle effect of environment on crack initiation is provided by the presence of surface films such as oxide layers and corrosion products. Two general effects are possible (20). If the film fractures under cyclic loading, fatigue cracks will invariably start into the substrate at the point of film rupture, and, in most cases, cause a reduction in total fatigue life. If the film does not rupture, then not only is the substrate protected from the environment but the film may actually exert a restraining force or near-surface dislocation activity. For the case of a dry anodic coating 1500 Å thick on a pure aluminum substrate, N_o was increased by a factor of 3 over the case of a dry, natural oxide coating 50 Å thick.

2.3 Crack Propagation

The observation of crack growth rates and their correlation with the crack tip stress intensity factor represents the first step toward quantifying our existing knowledge of the fatigue sequence. The first such empirical correlation was made by Paris and Erodogan (21) in 1963 and is generally expressed in the form

$$da/dN = A(\Delta K)^m \qquad [3]$$

where a is the instantaneous crack length, N the number of cycles, ΔK the stress intensity factor range, and A and m are material constants (m was set equal to 4 by Paris and Erodogan). The overriding importance of such an expression is that it can be used to calculate the number of cycles to propagate a preexisting flaw of size a_o to some critical length, a_f, at which failure will occur on the next load cycle, i.e.

$$N_f - N_o = \int_{a_f}^{a_o} \frac{da}{(da/dn)} \qquad [4]$$

The objective of most research in fatigue crack propagation today is to establish some quantitative relation such as eq.[4] and the conditions under which it is valid. Or, more basically, to establish the physical mechanism of crack growth so that a quantitative growth equation can be derived from first principles.

In the following discussion, we resort to the usual classifications of Stage I and Stage II crack growth (1). We find that Stage I cracking has been almost completely neglected despite the fact that in long-life fatigue it can consume over 90% of the life in ductile materials. The reason for this neglect is clear, however. The crack sizes in Stage I are very small, usually of the order of 1-2 grain sizes, and are correspondingly difficult to observe. Nevertheless, it is my belief that research into the mechanism and

rates of Stage I cracking represents one of the foremost frontiers in the search for fundamental knowledge of the fatigue process.

2.3.1 Stage I Crack Growth

We know that Stage I cracks propagate in a shear mode along crystallographic planes on which dislocation activity and density is high. Most of the information we have on the mechanisms of growth in Stage I derive from the happy circumstances that extensive Stage I fracture occurs in high strength nickel base alloy single crystals because of their highly planar slip nature (22). From this source and the studies by Kaplan and Laird (23), three possible mechanisms of Stage I growth have been proposed.

a) a plastic blunting mechanism similar to Stage II cracking (wavy slip mode materials).

b) an unslipping model, without rehealing at the crack tip (planar slip mode materials).

c) a decohesion model in which cyclic slip activity lowers the cohesive energy of the slip band or causes a local enhancement of the normal stress across the band by dislocation dipole accumulation.

None of these models have really been confirmed in a convincing way.

In the nickel-base alloys, the effect of raising the temperature during fatigue is to promote a transition to Stage II cracking (24). The effect of environment has also been investigated (25) for Mar-M200. Fatigue lives were ~ 3 times longer in vacuum (10^{-5} Torr) then in air. Electron fractography of the Stage I fracture surfaces showed that the gaseous environment (presumably oxygen) reduced the amount of plastic deformation during crack advance. The authors propose a model for Stage I cracking in which the gaseous environment lowers the surface energy, similar to (c), above.

Recently, Benson (26) has measured Stage I growth rates in single crystals of aluminum and finds a second power dependence on the strain concentration factor, Fig. 6. (The lower growth rate in air is presumably due to extensive crack branching on conjugate slip planes where tensile stresses aid cracking as a result of surface energy reduction in the moist air).

2.3.2 Stage II Crack Growth

The many contributing factors to Stage II crack growth have been largely sorted out in the past 3 years by experiments carried out in controlled environments. Baseline plots of log da/dN vs log ΔK obtained in an inert atmosphere or vacuum show these curves to consist of several regions. Figure 7 illustrates this fact schematically. Notice particularly the existence of a threshold ΔK below which da/dN is not measurable. Relating this threshold to the traditional endurance limit would be an interesting exercise! The changes in slope as ΔK increases illustrates why such a large range of values of the exponent m have been measured and indicates that the mechanism of growth probably changes as the slope goes through major changes. Finally, the effect of environment can be dramatic, and some of the data of Speidel, et. al. (27) are presented in Fig.8 to illustrate this fact. The sensitivity of the slope of the curves (and hence the exponent m) to environment indicates that environment has a strong effect on the mechanism of crack advance, a fact that can be readily discerned from fractographic studied of fatigued surfaces.

Although there is presently a large amount of activity in the investigation of environmental and elevated temperature effects on Stage II crack growth, the complexity and synergistic aspects of the problem qualify it as a difficult and important frontier for future

research. A fundamental need is to define the reduction in surface energy in terms of the non-equilibrium chemical potential of aggressive fluids. The effect of dynamic absorption or chemisorption on dislocation mobility at the surface also needs to be measured. The goal is a general prediction of environmental effects that transcends the treatment of each material and environment as a separate study.

A final word should be said about the sensitivity of Stage II crack growth rates to metallurgical properties. Several comparisons have been made between various steels and aluminum alloys using existing data. Hahn, et. al (28) found that crack growth rates for a given ΔK value in Fe-3Si steel (67 ksi yield strength) were not significantly different from those of five other low and medium strength grades of steel with different yield strengths. Bathias and Pelloux (29) have pointed out, however, that fatigue crack growth rates for $\Delta k > 30$ ksi $\sqrt{in}$. are an order of magnitude lower in steels with fcc structure than in bcc steels. For $\Delta k > 40$ ksi $\sqrt{in}$, the growth rates fall in the same scatter band with bcc steels.

Further evidence of the effect of microstructure on Stage II growth comes from the work of Ishii and Wertman (30). Figure 9 illustrates the effect of stacking fault energy on crack growth rates in single crystals with approximately the same orientation and ΔK at the tip. Although the yield stress (CRSS) increases with stacking fault energy and might account for the observed decrease in crack growth rates, earlier work by Miller, et. al (31) has essentially discounted this possibility. Hence, the slip mode of the material (wavy or planar) has an effect on da/dN, with planar slip mode materials producing the greatest resistance to crack growth.

3. The Application of Fundamental Knowledge to Technical Fatigue Problems.

In this section we will discuss the application of knowledge to two broad areas, materials improvement and life prediction under service loading.

3.1 Materials improvement

The subject of materials improvement and the approaches for achieving high fatigue strength have been discussed in detail quite recently (9,32,33). In this paper we discuss the problem generally and point out the more promising directions.

The application of fundamental knowledge to improve fatigue strength in materials has been disappointing in the sense that no new materials or alloys have appeared with an order of magnitude increase in fatigue strength. On the other hand our understanding of the fatigue process has provided useful guidelines for attacking the problem of materials development.

For example, the knowledge that most fatigue cracks start at the surface makes it obvious that surface treatments such as shot-peening and coating can only be effective in low-stress, long life fatigue where crack initiation is a significant fraction of total life. Moreover, the observation that inclusions can act both as crack starters and nuclei for additional crack growth within the plastic zone at the tips of existing cracks makes it obvious that their elimination would be advantageous over a wide range of fatigue lives. In fact, reduction of the volume fraction of undissolved second phases (inclusions) in 2024-T4 aluminum from 0.09% to 0.00016% produced a 60% increase in the number of cycles to initiate a crack and raised the fatigue strength of the alloy ~20% over the life range 10^5-10^7 cycles (9).

Fundamental knowledge of fatigue makes it clear that fatigue cracks start and grow at concentrations of plastic strain. Hence material microstructures which promote slip dispersal have long been considered desirable for fatigue resistance. In age-hardening aluminum alloys, such microstructures can be produced by introducing a dense and uniform dislocation forest through suitable thermo-mechanical treatments. In particular, Ostermann (34) has produced this microstructure in 7075 aluminum which increases the UTS by ~10% and the long life endurance limit by ~25 percent. If high purity 7075 is used, the endurance limit is increased by almost 50%.

Filament reinforced composite materials offer a different approach to fatigue resistant materials. The rationale here is that high modulus filaments can act as crack arrestors and reduce the amount of plastic deformation in the matrix. In fact the fatigue resistance of such composites as boron-epoxy and boron-aluminum are generally good, but the scatter in the fatigue data is quite large. This scatter is presumably due to either damaged filaments or uncontrolled interface microstructures. The design and development of fatigue resistant metal-matrix composite materials depends heavily on research to clarify the relation between interfacial microstructure and fracture resistance (35). One objective is the metallurgical design of interfaces e.g. well-bonded, plastic interfacial zones.

3.2 Life Prediction

Traditionally, fatigue life prediction has been based on experimentally determined stress amplitude vs life curves (so-called S-N curves) for smooth or notched specimens. As applications required that materials be stressed more and more into the inelastic or plastic range (e.g. thermal fatigue), the usefulness of strain amplitude-life curves became apparent. Initially, these curves were plotted as the logarithm of the plastic strain range $\Delta\varepsilon_n/2$, versus log N_f. Such a plot results in a straight line, now known as the Manson-Coffin law, which is used extensively to describe low cycle fatigue of many materials.

A more useful way of plotting life data today is in terms of total strain vs life, Fig.10. In this way, both the plastic and elastic regimes can be included on one diagram. The curve breaks into essentially two linear plots: the plastic strain Manson-Coffin Law and the elastic strain Basquin relationship. The point at which the elastic and plastic strains are equal has been defined as the transition fatigue life, N_T, and serves as a useful definition of the quantitative boundary between low and high cycle fatigue. An empirical equation can be written (36) which describes the entire curve of Fig. 10

$$(\Delta\varepsilon/2) = (\Delta\varepsilon_e/2) + (\Delta\varepsilon_p/2) = (\sigma'_f/E)(2N_f)^b + \varepsilon'_f(2N_f)^c \quad [5]$$

where the parameters in the equation are σ'_f = fatigue strength coefficient, ε'_f = fatigue ductility coefficient, E is Young's modulus, and N_f is the number of cycles to failure. ($2N_f$ is the number of reversals to failure).

This representation of constant strain amplitude life data has proven extremely useful for materials selection (37), for preliminary design of component structures, and more especially as a basis for at least one, cumulative damage analysis procedure (cf. 3.2.1).

3.2.1 Load interaction effects

Virtually all real structures, which are subject to fatigue failure, experience variable amplitude loading. It is the concensus of all those who are active in fatigue research today that the study

of load interaction effects on fatigue mechanisms is the single most important frontier yet to be explored in a fundamental way. At the present time our knowledge is only sufficient to say that "fatigue life predictions for practical load-time histories should be based on tests with practical load sequences."*

Two approaches for applying fundamental knowledge to this vexing problem are now being vigorously explored. Both are semi-empirical. The first makes use of a cycle by cycle determination of the cyclic stress-strain response (hysteresis loop), of a material under variable amplitude loading. These responses are then combined with a constant amplitude life equation such as Eq.[5] so that the damage may be summed linearly (38,39). The second approach treats the fatigue sequence as composed entirely of crack propagation, and expressions for da/dN are appropriately summed over all load amplitudes.

3.2.2 Creep-Fatigue Interactions

As high temperature applications of materials multiply, the problem of life prediction under combined conditions of fatigue and creep becomes more accute. It is again a consensus among active workers in fatigue that this area represents a very important frontier for gaining fundamental knowledge regarding the creep-fatigue interaction. Very little work has been reported that would enable one to formulate any type of mechanistic model of the interaction. Manson (40) has proposed an empirical method of dealing with the problem (strain-range partitioning) which has much in common with the cyclic stress-strain approach to load interaction discussed in 3.2.1.

*J. Schijve

4. General Conclusions

This general overview of our fundamental knowledge of fatigue and the research frontiers which exist has shown the greatest need for future research to be in quantifying that which we already know in a qualitative way. Some specific frontiers are:

- Development of a quantitative theory of fatigue hardening
- Understanding and predicting the stability of metallurgical and dislocation microstructures under cyclic loading
- Documentation of the effects of strain rate and temperature on cyclic stress-strain response
- Developing a model for crack initiation in high strength materials, particularly in long life fatigue
- Determining the effects of environment of the rate of crack inititiation
- Determination of the mechanisms and rates of Stage I fatigue crack growth as a function of temperature, environment and material properties
- General prediction of the effect of environment-material couples on Stage II crack growth rates
- Definition of the structure-sensitive aspects of Stage II crack growth rates
- General study of load interaction effects on the fundamental mechanisms of the fatigue sequence
- General study of creep-fatigue interactions and their effect on fundamental mechanisms of fatigue

In all cases, experiments ought to be devised realistically, so that the results may be eventually applied to the improvement of materials and the prediction of fatigue lives under complex

conditions. After all, it is these very practical problems which give the stimulus for continued work in the whole field of fatigue research.

5. Acknowledgements

This paper could not have been written without the help and advise which the author solicited from numerous people. Although I take full responsibility for this written version, I want to acknowledge with thanks the willingness of the following people to share with me their ideas and their hopes for the future of fatigue research: A. S. Argon, L. F. Coffin, D. J. Duquette, C. E. Feltner, Henry Fuchs, H. Grover, G. T. Hahn, J. R. Hancock, H. F. Hardrath, H. D. Nine, C. Laird, P. Lukas, A. J. McEvily, S. S. Manson, P. Neumann, R. M. Pelloux, W. H. Reimann, J. Schijve, B. Tomkins, R. P. Wei, S. Weissmann, C. H. Wells, and W. A. Wood.

References

1. J. C. Grosskreutz, phys. stat. sol. (b) 47, 11, 359 (1971).
2. W. J. Plumbridge and D. A. Ryder, Metallurgical Reviews 14, 119 (1969).
3. R. W. Landgraf, Ford Motor Company, Scientific Laboratory, Dearborn, Michigan.
4. P. Lukas and M. Kleanil, phys. stat. sol. (in press).
5. M. Ruhle, phys. stat. sol. 26, 661 (1968).
6. J. Piqueras, J. C. Grosskreutz and W. Frank, phys. stat. sol. (a) 11, 567 (1972).
7. W. Frank, M. Ruhle, and M. Saxlova, phys. stat. sol. 26, 671 (1968).
8. H. Mughrabi, Max Planck Inst. f. Metallforschung. Stuttgart (private communication).

9. J. C. Grosskreutz in Fatique and Fracture of Aircraft Structures and Materials, Air Force Flight Dynamics Laboratory TR 70-144 (Wright-Patterson Air Force Base, Ohio) p.47 (1970).

10. P. Neumann, Z. Metallkunde 59, 927 (1968).

11. P. Neumann, Acta Metallurgica 19, 1233 (1971).

12. J. R. Hancock and D. K. Benson, Midwest Research Inst., Kansas City, Mos. (private communication).

13. B. Tomkins, Phil. Mag. 18, 1041 (1968).

14. Fatigue at Elevated Temperature, Special Technical Publication (ASTM), in press (1973).

15. C. Laird and D. J. Duquett in Corrosion Fatigue, National Association of Corrosion Engineers (1972) (in press).

16. J. C. Grosskreutz, "Mechanisms of Fatigue in 7075-T6 Aluminum," AFML-TR-66-96, Wright Patterson Air Force Base, Ohio (1966).

17. D. K. Benson, J. C. Grosskreutz and G. G. Shaw, Met. Trans. 3, 1239 (1972).

18. Douglas E. MacDonald and W. A. Wood, J. Inst. of Metals, 100, 73 (1972).

19. C. H. Wells, C. P. Sullivan and M. Gell, in Metal Fatigue Damage, Special Technical Publication No. 495 (ASTM, Philadelphia, Pa.) p.61 (1971).

20. J. C. Grosskreutz, in Corrosion Fatigue, National Association of Corrosion Engineers, Houston, Texas 1972 (in press).

21. P. C. Paris and F. Erodogan, J. Basic Eng. 85, 528 (1963).

22. M. Gell and G. R. Leverant, Acta Metallurgica 16, 553 (1968).

23. H. I. Kaplan and C. Laird, Transactions of the Met. Soc. AIME 239, 1017 (1967).

24. M. Gell, G. R. Leverent and C. H. Wells, in High Fatigue Resistance in Metals and Alloys, Special Technical Publication No. 467 (ASTM, Philadelphia, Pa.) p.113 (1970).

25. D. J. Duquette and M. Gell, Met. Trans. 2, 1325 (1971).

26. D. K. Benson, Midwest Research Institute, Kansas City, Mo. (private communication).

27. M. O Speidel, M. J. Blackburn, T. R. Beck and J. A. Feeney in Corrosion Fatigue, National Association of Corrosion Engineers Houston, Texas (1972).

28. G. T. Hahn, R. C. Hoagland, and A. R. Rosenfield, Met. Trans. 3, 1189 (1972).

29. C. Bathias and R. M. Pelloux, "Fatigue Crack Propagation in Martensitic and Austenitis Steels", MIT Rept. dated Marck 1972, Dept. of Metallurgy and Materials Science.

30. H. Ishii and J. Weertman, Met. Trans. 2, 3441 (1971).

31. G. A. Miller, D. H. Avery and W. A. Backofen, Trans. TMS-AIME, 236, 1667 (1966).

32. Achievement of High Fatigue Resistance in Metals and Alloys, Special Technical Publication No. 467 (ASTM, Philadelphia, Pa.) (1970).

33. J. C. Grosskreutz, Met. Trans. 3, 1255 (1972).

34. F. Ostermann, Met. Trans. 2, 2897 (1971).

35. J. R. Hancock, "Fatigue of Boron-Aluminum Composites," Midwest Research Institute, Kansas City, Mo. (to be published, 1972).

36. R. W. Landgraf, in High Fatigue Resistance in Metals and Alloys, Special Publication No. 467, (ASTM, Philadelphia, Pa. p.3 (1970).

37. C. E. Feltner and R. W. Landgraf, J. Basic Engineering, Trans ASME 93, 44 (1971).

38. R. W. Landgraf and R. M. Wetzel, "Cyclic Deformation and Fatigue Damage," International Conference on Mechanical Behavior of Materials, Kyoto, Japan, 1971. (See also Ford Scientific Staff preprint dated April 13, 1972).

39. R. M. Wetzel, "A Method of Fatigue Damage Analysis, " Ford Scientific Research Staff preprint dated September 1971.

40. S. S. Manson in Fatigue at Elevated Temperature, Special Technical Publication (ASTM) in press (1973).

Figure Captions

Fig. 1 Cyclic and montonic stress-strain curves (R. W. Landgraf, ref. 32).

Fig. 2 Transmission electron micrograph of the primary glide plane of fatigue-hardened copper. Mobile dislocations are seen lying between cell boundaries. Sample neutron-irradiated under load at 4°K with $2x10^{18}$ neut/cm^2. (Courtesy H. Mughrabi).

Fig. 3 Plot of the cyclic strain hardening exponent, n', *versus* strain rate for 7075-T6 Al. (Courtesy J. R. Hancock and D. K. Benson.

Fig. 4 Cyclic stress-strain curves for 20/25/Nb stainless steel at various temperatures. (After Tomkins, Ref. 14).

Fig. 5 "Slipless" crack in a grain of fatigued titanium. Length of crack is ~10 μm. (Ref. 18).

Fig. 6 Stage I crack growth rates in aluminum single crystals. (Courtesy D. K. Benson).

Fig. 7 Schematic representation of Stage II crack growth rate *vs.* ΔK, the stress intensity factor range.

Fig. 8 Effect of several environments on crack growth rates in 7079-T651 aluminum alloy. (Ref. 27).

Fig. 9 Fatigue crack growth rate *vs.* stacking fault energy and critical resolved shear stress for single cr stals of Cu-Al alloys. (Ref. 30).

Fig.10 Schematic representation of strain-life relation.

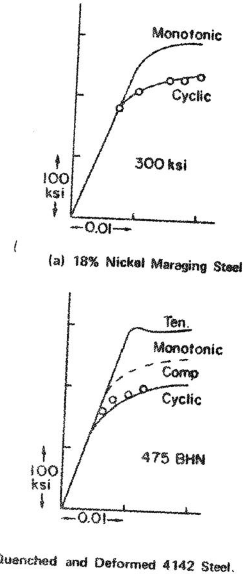

Fig. 1

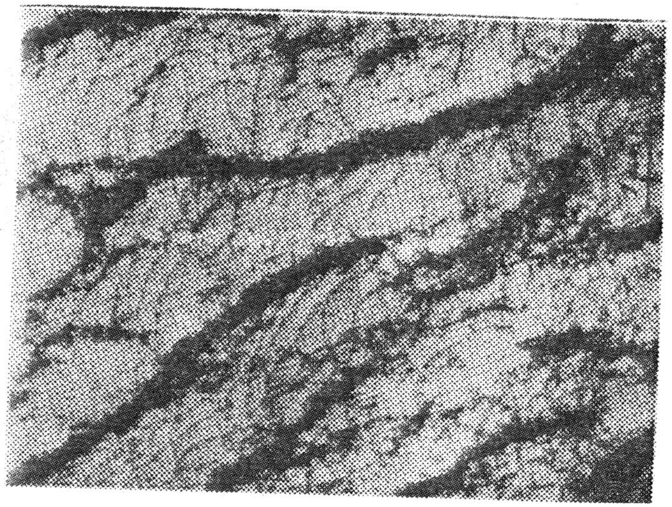

Fig. 2

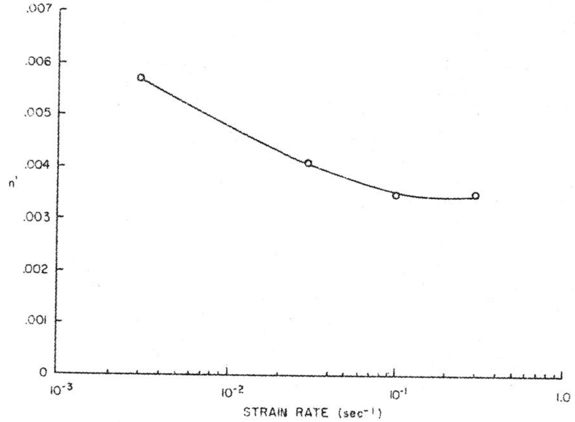

Fig. 3

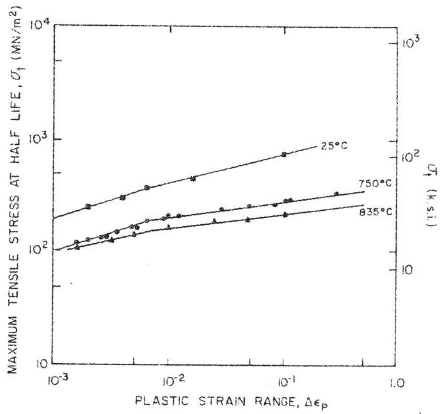

Fig. 4

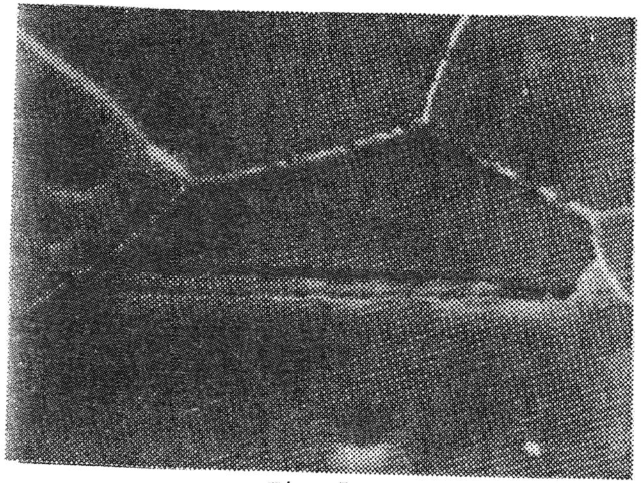

Fig. 5

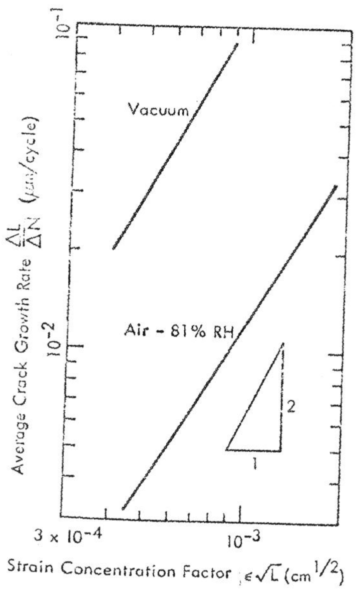

Fig. 6

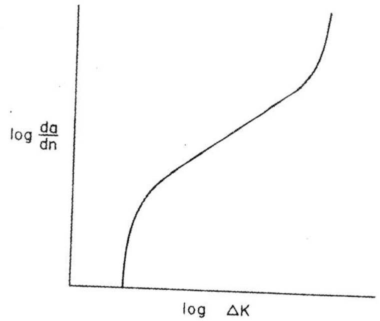

Fig. 7

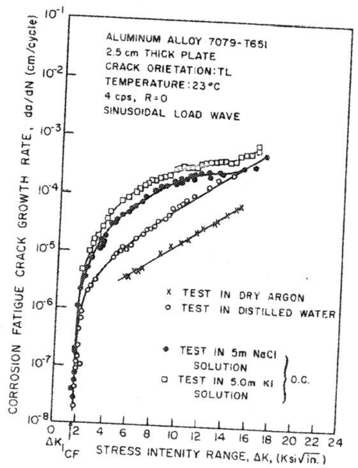

Fig. 8

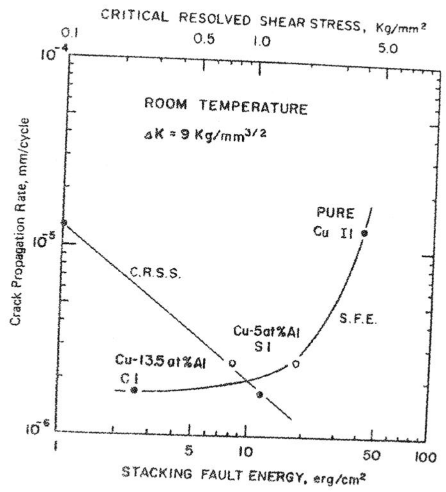

Fig. 9

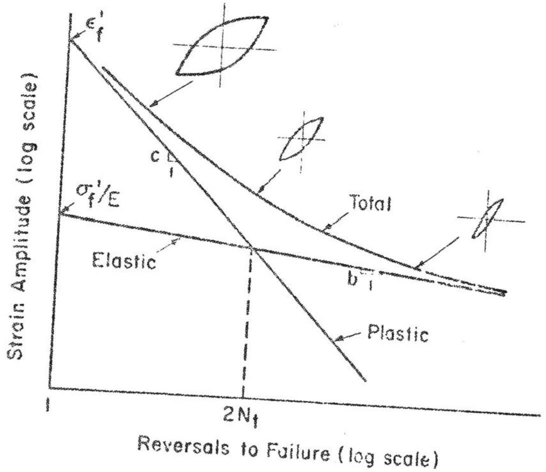

Fig. 10

PL V-212